THE JOURNAL OF PHYSICAL CHEMISTRY C

Article

pubs.acs.org/JPCC

Carbon Dioxide Capture from Air Using Amine-Grafted Porous Polymer Networks

Weigang Lu,[†] Julian P. Sculley,[†] Daqiang Yuan,[‡] Rajamani Krishna,[§] and Hong-Cai Zhou*[,†]

[†]Department of Chemistry, Texas A&M University, College Station, Texas 77843, United States

[‡]State Key Laboratory of Structure Chemistry, Fujian Institute of Research on the Structure of Matter, Chinese Academy of Sciences, Fuzhou, Fujian, 350002, China

[§]Van't Hoff Institute for Molecular Sciences, University of Amsterdam, Science Park 904, 1098 XH Amsterdam, The Netherlands

Supporting Information

ABSTRACT: Amine-grafted porous polymer networks were investigated for CO_2 capture directly from air (400 ppm CO_2, 78.96% N_2, and 21% O_2). Under these ultradilute conditions, PPN-6-CH_2DETA has an extraordinarily high CO_2 selectivity (3.6×10^{10}) and loading capacity (1.04 mol/kg) as calculated using ideal adsorption solution theory. In addition we have shown that the material outperforms other materials based on simulated breakthrough calculations, thus showing great potential to be used in direct air capture applications.

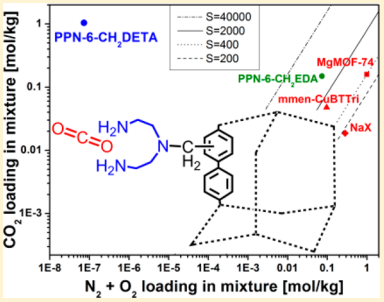

Rising atmospheric CO_2 levels have been strongly correlated with global climate change. Current levels are about 392 ppm and rising as we continue to consume extraordinary quantities of fossil fuels to feed societies' voracious and growing appetite for energy.[1] Scientists around the world are investigating new materials and processes to mitigate CO_2 emissions by implementing capture technologies, primarily at large single-point sources such as power plants, which are generating about one-third of total CO_2 emissions in relatively high concentrations (5−20% in exhaust gas).[2] This focus will allow significant quantities of CO_2 to be captured, therefore slowing the rise in global levels. These new technologies are extremely important as we will continue to burn substantial quantities of fossil fuels over the next decades, despite tremendous efforts in alternate, cleaner fuel sources. It has, however, been suggested that, in addition to stalling emissions, we need to begin capturing CO_2 directly from the air.[3,4] This would additionally address the other two-thirds of emissions that are generated from the transportation and other industries (e.g., concrete, paper, and chemical production). From a technology standpoint, direct air capture (DAC) poses an even greater challenge because of the extremely dilute CO_2 concentrations in ambient air. However, DAC provides some interesting economic benefits that may aid in making this a viable global technology. Among the largest factors are that it can be decoupled from the fossil fuel power generation, thus taking advantage of renewable energy resources to drive the regeneration process, and allowing deployment directly at sequestration sites, substantially reducing CO_2 transport costs.[5] In fact, CO_2 capture from ambient air has already been deployed in a few scenarios and is a crucial part of daily operations. Scrubbers are being implemented as part of life support systems in submarines, spacecrafts, and personal closed-circuit breathing systems, where CO_2 concentrations are typically below 5000 ppm, the United States Occupational Safety and Health Administration's threshold limit. If the exhaled gas is to be recycled, it is necessary to remove the CO_2 from the breathing loop to avoid its presence at concentrations considered hazardous to human health.

All of these closed systems provide added benefits over global scale DAC: they have 1 order of magnitude higher CO_2 concentrations, known and manageable contaminant levels, and the entire volume of gas can be directed through scrubber units because they are completely enclosed systems. For larger scale applications, movement of air through the scrubber units becomes an important energy consideration, although wind may be used to facilitate transport.

One well-studied DAC technology uses sodium hydroxide solutions to absorb CO_2 from air and convert it to sodium carbonate, which is further reacted with $Ca(OH)_2$ to form calcium carbonate ($CaCO_3$(s)). The CO_2 is recovered via a calcination step by heating to >900 °C, forming CaO as the solid product; this process is obviously quite energy intensive, and has been estimated by an American Physical Society report to be around $600 per ton of CO_2.[6] Another state of the art technology relies on amine solutions to chemically react with CO_2, forming carbamates, which has the benefit of being selective for only CO_2 over all of the other gases. In both processes, however, there are some significant drawbacks,

Received: November 21, 2012
Revised: January 24, 2013
Published: January 28, 2013

   dx.doi.org/10.1021/jp311512q | J. Phys. Chem. C 2013, 117, 4057−4061

particularly, large energy requirements to regenerate the system, highly corrosive solutions, and solvent boil-off, all of which can pose significant problems during extended operation.[7]

To combat the drawbacks, an alternate approach, capturing CO_2 in solid sorbents via a physical adsorption mechanism, have been proposed and developed.[3,8−10] These systems must have high selectivities for CO_2 over other gases at the concentrations at which separation is to be performed, large working capacities, low regeneration energies, and stability toward contaminants. Recently, amine-tethered porous silica composites[11−14] and amine-appended metal−organic frameworks (MOFs), such as mmen-Mg_2(dobpdc),[15,16] have shown promising results to capture CO_2 from ultradilute gas streams. A detailed economic study of DAC by Kulkarni and Sholl recently reported the total system cost at several potential U.S. sites to be around \$100/ton of CO_2.[5] The solid sorbent chosen for their study, TRI-PE-MCM-41, has a loading of 0.98 $mol_{CO2}/kg_{sorbent}$ and a calculated heat of adsorption of 67.3 kJ/mol.[8] One of the conclusions they reached is that higher loading may further reduce this cost, as larger volumes of CO_2 can be extracted per adsorption cycle. The regeneration energy is largely dependent on the heats of adsorption and heat capacities of the materials.

The results presented herein focus on tethering amines to porous polymer networks (PPNs). The support structure, PPN-6, is a covalently bonded carbon scaffold with a BET surface area of 4023 m^2/g, which is extremely stable toward strong acid and base. This stability and large internal pore surface have allowed us to modify the structure by introducing sulfonic acid groups[17] and, in this case, amines to make this material suitable in a DAC process.

EXPERIMENTAL SECTION

The materials discussed herein were synthesized as previously reported.[18] Experimental single-component isotherms for CO_2, N_2, and O_2 are shown in the Supporting Information (Figures S1−S5). These isotherms are first converted from excess loadings to absolute loadings, using the Peng−Robinson equation of state for estimation of the fluid density inside the pores at the relevant temperatures and pressures.

RESULTS AND DISCUSSION

Isotherm Fit. N_2 and O_2 adsorption isotherms of all of the structures analyzed, as well as the CO_2 isotherm of PPN-6-CH_2Cl, show no isotherm inflections, thus allowing the use of a single-site Langmuir model to fit the data. The CO_2 adsorption isotherms for PPN-6-CH_2DETA and −EDA, however are much steeper in the low-pressure regime and therefore require a multisite Langmuir model to properly fit the data. Fitting of these adsorption isotherms in the low-pressure regions are of particular importance in the context of CO_2 capture from ambient air because of the low concentrations of about 400 ppm. In our earlier work, which examined CO_2 capture from flue gases, dual-site Langmuir fits were used. The isotherms were carefully remeasured at very low pressures and revealed a second inflection point, thus indicating the need for a triple-site model:

$$q^0 \equiv q_A^0 + q_B^0 + q_C^0 = \frac{q_{sat,A} b_A p}{1 + b_A p} + \frac{q_{sat,B} b_B p}{1 + b_B p} + \frac{q_{sat,C} b_C p}{1 + b_C p} \quad (1)$$

It is vital for the isotherm fits to properly capture the steep isotherm characteristics at pressures below 1000 Pa. Each of the sites contributes to the total loading at different pressures. For CO_2 capture from ambient air, the parameters for the first site are of particular importance in determining the component loadings in mixtures with N_2 and/or O_2 because the partial pressures of CO_2 are extremely low. The fitted parameters for all isotherms are given in the respective tables in the Supporting Information.

In the context of this discussion, we would like to make a note about fitting experimental data to conform to physical models. It is important to keep in mind the chemical and structural characteristics of the system that is being modeled before adding fitting parameters. Theoretically, any isotherm can be modeled by an n-site Langmuir model; however, when using the Langmuir model to represent reality, structural data should be taken into account. In the case of PPN-6-CH_2DETA and −EDA a three-site model is appropriate because the chemical structure of these materials is made up of primary and secondary amines, and the backbone (phenyl) moieties, all of which have been shown to have different adsorption enthalpies with CO_2. Using more fitting parameters could increase the goodness-of-fit for each isotherm, but would chemically not make sense, thus making a three-site model the appropriate choice.

Another point, which has not been properly addressed in some published papers using multisite Langmuir models to fit CO_2 data, is the definition of the q_{sat} and b parameters. When these values are fit using minimization functions, there is the possibility of reaching a local minimum, but one that does not conform to good chemical sense. Therefore, when fitting the q_{sat} values over a range of temperatures, the q_{sat} value should be fixed. By definition, q_{sat} describes the quantity of gas adsorbed when exactly one layer of a given site is saturated, which is not temperature-dependent. The b values can be thought of as adsorption-equilibrium constants, generally decreasing with temperature, and can often be modeled by the Arrhenius equation. These minor nuances when fitting experimental data can have significant positive or negative effects on the predicted loadings and any subsequent calculations.

IAST Calculation. Ideal adsorption solution theory (IAST), developed by Myers and Prausnitz,[19] has frequently been used to evaluate mixed component isotherms because it has been shown to reflect true mixed component measurements. To evaluate the efficacy of using PPN-6-CH_2EDA and −DETA for DAC, two separate IAST evaluations were performed. In both cases, CO_2 concentrations were taken to be close to the current global level of 400 ppm (40 Pa). The first set of calculations was performed using N_2 as the balance gas (100 kPa); the results are shown in Table S6. In previous studies it has been shown that O_2 can play a significant role in competing for adsorption sites against CO_2. To ensure a higher degree of accuracy, we additionally tested the effects of O_2 in our systems. The second set of calculations was performed using "air" to be composed of 78.96% N_2 and 21% O_2; the data are plotted in Figure 1. The results show that O_2 plays a larger role in competition with CO_2 than N_2 does; however, PPN-6-CH_2DETA retains significant adsorption of CO_2 in the mixture, thus indicating its efficacy for DAC. The reasons for the high selectivity over both N_2 and O_2 can be ascribed in large part to the high CO_2 loadings, particularly below 100 Pa. Other materials for CO_2 capture, Mg-MOF-74, NaX zeolite, and

dx.doi.org/10.1021/jp311512q | J. Phys. Chem. C 2013, 117, 4057−4061

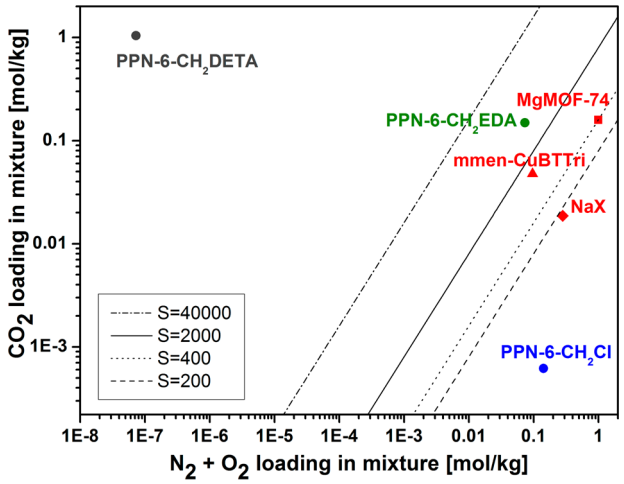

Figure 1. IAST calculations of component loadings of CO_2 and (N_2 + O_2) in the adsorbed phase with selected materials. The total bulk gas pressure is 100 kPa and contains 400 ppm CO_2, 78.96% N_2, and 21% O_2. Loadings for calculated selectivities are shown as a guide.

mmenCuBTTri are plotted for comparison, although only results using CO_2/N_2 are available.[20,21]

Comparing the two amine-grafted PPNs reveals significant differences in CO_2 loading at these low concentrations. −EDA and −DETA have both been shown to be possible candidates for flue gas capture because of high selectivities and loading capacities in mixed component systems; however, for ambient air capture only −DETA is a viable candidate. The reasons for this have a strong basis in the chemical structure of the two materials. The −EDA structure has only short diamine chains, whereas −DETA has a third amine available to bind CO_2. This structural difference imparts −DETA with much higher loading without any pore blockage. The high loading and chemisorption-type interactions result in a boost in selectivity of 7 orders of magnitude. This difference is difficult to compare because the selectivity for −DETA is so high. A more telling number is the resultant purity of gas after separation (Table 1, eq 6 in Supporting Information). The value for −EDA is 67.0% in the N_2 + O_2 case, whereas −DETA reaches 99.999993%, which indicates that this material would be useful in a true mixed component system because the resulting CO_2 is a high enough purity to compress and store or use as a UHP grade chemical commodity. The desorption, or recovery, of this high-purity gas also does not require extraordinary amounts of energy, which is evidenced by the moderate heats of adsorption of 54 kJ/mol. See Figure S6 for loading-dependent adsorption enthalpies of all materials.

Table 1. Comparison of CO_2 Loading, IAST Selectivity, and CO_2 Purity Data for CO_2 Capture from "Air" Containing 400 ppm CO_2

		N_2[a]		N_2 + O_2[a]	
material	CO_2 (mol/kg)	S_{IAST}	purity	S_{IAST}	purity
MgMOF-74[20]	0.16	401	13.8		
Zeolite NaX[20]	0.02	166	6.2		
mmen-CuBTTri[21]	0.05	1239	33.1		
PPN-6-CH_2Cl	0.001	11	0.4	11	0.4
mmen-Mg_2(dobpdc)[15]	2.05	4.9×10^{4}[b]	96.1	4.2×10^{4}[b]	94.4
PPN-6-CH_2EDA	0.15	5078	67.0	5086	67.0
PPN-6-CH_2DETA	1.04	3.8×10^{10}	99.9	3.6×10^{10}	99.9

[a]Balance gas. [b]"Molar selectivity".

For PPN-6-CH_2DETA, pure component loading at 40 Pa is not as high as that for mmen-Mg_2(dobpdc);[15] however, it is a decidedly better choice for CO_2 capture from ambient for several reasons: (1) The selectivity over N_2 and O_2 are substantially higher, although the values are extraordinarily high (3.6×10^{10} vs 4.2×10^{4}) in both cases. (2) A more meaningful method of evaluating these compounds for ambient air capture is the modeled CO_2 purity after capture, reaching only 94% (below the industrial standard for pure gas) in the N_2 + O_2 case for mmen-Mg_2(dobpdc). Further comparisons are listed in Table 1. (3) Stability, primarily toward water, will also be a significant factor when extracting CO_2 from ambient air. While MgMOF-74 has been shown to be unstable toward moisture,[22] amine-containing materials have been reported to enhance sorption capacities and selectivities in the presence of water.[8,13,23,24]

Breakthrough Calculation. To determine whether −DETA is indeed a promising candidate for CO_2 removal from ambient air in fixed bed adsorbers, breakthrough calculations were performed using the methodology described in earlier works.[25] The breakthrough simulation used here has been validated by comparison with experimental breakthrough measurements carried out using a variety of mixtures by two different groups.[26−28] This analysis provides crucial insights into true performance because it takes working capacity, selectivity, sorbent volume, and loading in mixed conditions into account. A schematic of a packed bed adsorber and full description of equations and methodology are given in the Supporting Information. Results of breakthrough calculations and comparison to other materials are shown in Figure 2a. The breakthrough calculations were carried out in both scenarios (using air to be 99.96% N_2, or a mixture of 78.96% N_2 and 21% O_2), keeping the constant 400 ppm inlet partial pressure of CO_2. The *x*-axis is a *dimensionless* time, τ, obtained by dividing the actual time by the contact time between the gas and the porous materials. Concentration of CO_2 in the outlet gas (ppm) is plotted along the *y*-axis. The result of a desirable material is longer breakthrough times, τ_{break}, as this allows more CO_2 to be adsorbed. From a practical point of view, the best structure is the one that is capable of adsorbing the most amount of CO_2 for a given volume of material. The quantity adsorbed by the material in the packed column during the time interval $0 - \tau_{break}$ is expressed in moles of CO_2 adsorbed per liter of adsorbent material and is plotted on the *y*-axis of Figure 2b. PPN-6-CH_2Cl has the shortest breakthrough time because it has the lowest CO_2 adsorption capacity, while −DETA has the longest breakthrough time, reflecting the highest uptake capacity of CO_2.

At the time of breakthrough, CO_2 uptake of −DETA is 0.36 mol/L, compared with 0.12 mol/L for MgMOF-74. Although MgMOF-74 has been shown to be useful for flue gas capture, in large part because the adsorption capacity at 0.15 bar is so high, at lower concentrations, such as ambient air, −DETA is, to the best of our knowledge, superior to any other materials tested by IAST and simulated breakthrough methods to date.

Working Capacity. By fitting experimental data to a multisite Langmuir model, adsorption quantities can be modeled as a function of pressure and temperature. Working capacity of a material in a TSA process can be defined as the

dx.doi.org/10.1021/jp311512q | J. Phys. Chem. C 2013, 117, 4057−4061

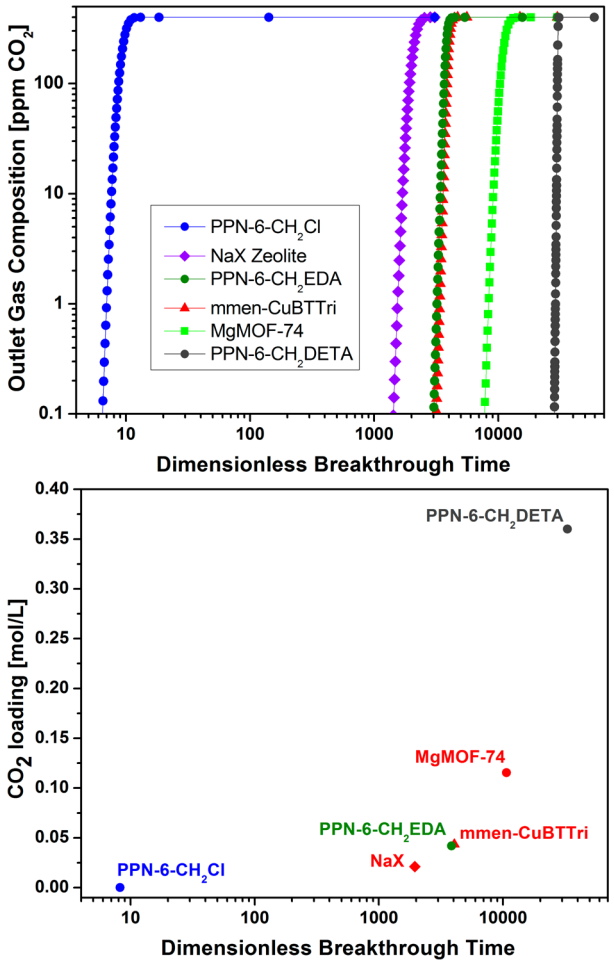

Figure 2. (a) Transient breakthrough of a $CO_2/N_2/O_2$ mixture in an adsorber bed packed with $-CH_2Cl$, $-EDA$, $-DETA$, MgMOF-74, NaX zeolite, and mmenCuBTTri. (b) CO_2 adsorption capacities expressed as moles of CO_2 adsorbed per liter of adsorbent material as a function of the dimensionless breakthrough times.

difference in loading quantities at the adsorption and desorption state (eq 2):

$$\sum q_{\mathrm{sat},i} \frac{b_i(T_{\mathrm{ads}})P_{\mathrm{ads}}}{1 + b_i(T_{\mathrm{ads}})P_{\mathrm{ads}}} - \sum q_{\mathrm{sat},i} \frac{b_i(T_{\mathrm{des}})P_{\mathrm{des}}}{1 + b_i(T_{\mathrm{des}})P_{\mathrm{des}}} \qquad (2)$$

where q_{sat} and b are Langmuir parameters (see Supporting Information for details) and i is the index for the CO_2 adsorption site.

Working capacities were calculated from mixed component (IAST) loadings at 295 K/400 ppm CO_2 and desorption at 1 bar over a range of temperatures. Figure 3 shows the working capacities of DAC as a function of temperature, with positive working capacities above 98 °C. Porous materials generally have low heat capacities and in the case of $-DETA$, the adsorption enthalpies are around 60 kJ/mol (see Figure S6), indicating that the regeneration energy penalty would not be very high.

CONCLUSIONS

DAC is a viable technology that should be given more consideration, as several features make it economically more feasible than it is often given credit for. The primary concerns regarding costs of DAC are driven by high regeneration

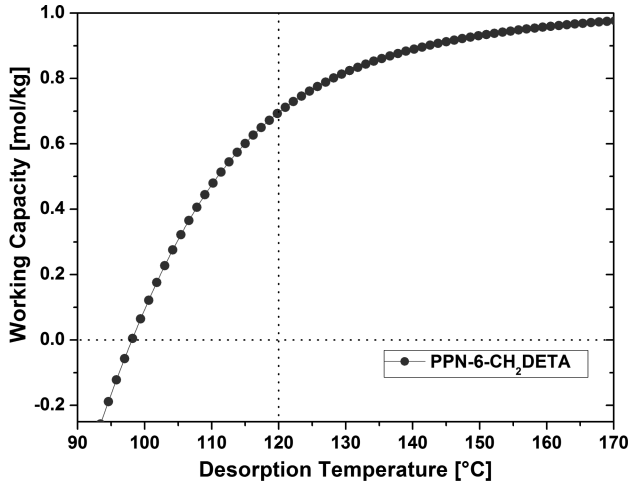

Figure 3. Working capacity as a function of desorption temperature.

energies for the state of the art technologies, in large part because of the enormous quantities of water that must be heated during regeneration. By moving to solid sorbent technologies, these energy penalties can be reduced. Amines supported on solid materials have been explored, primarily on silica supports; however, to the best of our knowledge, these amine-grafted PPNs represent the first sorbents taking advantage of highly porous three-dimensional carbon scaffold.[3,10] Due to the stability of the base structure and large internal pore volume, many different amines can be included and amine loadings could easily be varied to tune the adsorption properties toward DAC. To the best of our knowledge, at 400 ppm, PPN-6-CH_2DETA has among the highest selectivity and loading capacities using IAST and simulated breakthrough measurements of any compound reported to date. We can also conclude that the length of the amine chain is of crucial importance, as the shorter amine, $-EDA$, did not perform well under the conditions tested. $-DETA$ has a 6% higher CO_2 loading capacity than TRI-PCM-40 at 400 ppm (0.98 mol/kg) and the heat of adsorption is also evaluated to be about 25% lower (53.8 vs 67.3 kJ/mol). Both of these factors were significant parameters identified by Kulkarni and Sholl as large contributors to the capture cost in their recent report. This leads us to conclude that low costs are readily achievable with the $-DETA$ framework. Work is still being conducted on further extending the amine chains and varying loading ratios as this has been shown to affect CO_2 loading.

ASSOCIATED CONTENT

Supporting Information

Isotherm fit, IAST calculation, and breakthrough calculation. This material is available free of charge via the Internet at http://pubs.acs.org.

AUTHOR INFORMATION

Corresponding Author

*Tel.: 979-422-6329. Fax: 979-845-1595. E-mail: zhou@mail.chem.tamu.edu

Author Contributions

The manuscript was written through contributions of all authors. All authors have given approval to the final version of the manuscript. W. Lu and J. P. Sculley contributed equally.

dx.doi.org/10.1021/jp311512q | J. Phys. Chem. C 2013, 117, 4057−4061

Funding

This work was entirely supported by the U.S. Department of Energy as part of the Center for Gas Separations Relevant to Clean Energy Technologies, an Energy Frontier Research Center funded by the U.S. DOE, Office of Science, Office of Basic Energy Sciences under Award Number DE-SC0001015.

Notes

The authors declare no competing financial interest.

■ ACKNOWLEDGMENTS

We would like to thank W.M. Verdegaal for his helpful discussions.

■ REFERENCES

(1) National Oceanic and Atmospheric Administration. Trends in Atmospheric Carbon Dioxide. http://www.esrl.noaa.gov/gmd/ccgg/trends/global.html. Accessed Apr 5, 2012.

(2) MacDowell, N.; Florin, N.; Buchard, A.; Hallett, J.; Galindo, A.; Jackson, G.; Adjiman, C. S.; Williams, C. K.; Shah, N.; Fennell, P. An overview of CO_2 capture technologies. *Energy Environ. Sci.* **2010**, *3*, 1645−1669.

(3) Jones, C. W. CO_2 Capture from Dilute Gases as a Component of Modern Global Carbon Management. *Annu. Rev. Chem. Biomol. Eng.* **2011**, *2*, 31−52.

(4) Lackner, K. S.; Brennan, S.; Matter, J. M.; Park, A.-H. A.; Wright, A.; van der Zwaan, B. The urgency of the development of CO_2 capture from ambient air. *PNAS* **2012**, *109*, 13156−13162.

(5) Kulkarni, A. R.; Sholl, D. S. Analysis of Equilibrium-Based TSA Processes for Direct Capture of CO_2 from Air. *Ind. Eng. Chem. Res.* **2012**, *51*, 8631−8645.

(6) Socolow, R. H. et al. *A Technology Assessment for the APS Panel on Public Affairs*; American Physical Society: College Park, MD, June 1, 2011.

(7) Sumida, K.; Rogow, D. L.; Mason, J. A.; McDonald, T. M.; Bloch, E. D.; Herm, Z. R.; Bae, T. H.; Long, J. R. Carbon Dioxide Capture in Metal−Organic Frameworks. *Chem. Rev.* **2012**, *112*, 724−781.

(8) Belmabkhout, Y.; Serna-Guerrero, R.; Sayari, A. Amine-bearing mesoporous silica for CO_2 removal from dry and humid air. *Chem. Eng. Sci.* **2010**, *65*, 3695−3698.

(9) Choi, S.; Gray, M. L.; Jones, C. W. Amine-Tethered Solid Adsorbents Coupling High Adsorption Capacity and Regenerability for CO_2 Capture From Ambient Air. *ChemSusChem* **2011**, *4*, 628−635.

(10) Choi, S.; Drese, J. H.; Jones, C. W. Adsorbent Materials for Carbon Dioxide Capture from Large Anthropogenic Point Sources. *ChemSusChem* **2009**, *2*, 796−854.

(11) Chaikittisilp, W.; Khunsupat, R.; Chen, T. T.; Jones, C. W. Poly(allylamine)−Mesoporous Silica Composite Materials for CO_2 Capture from Simulated Flue Gas or Ambient Air. *Ind. Eng. Chem. Res.* **2011**, *50*, 14203−14210.

(12) Chaikittisilp, W.; Kim, H.-J.; Jones, C. W. Mesoporous Alumina-Supported Amines as Potential Steam-Stable Adsorbents for Capturing CO_2 from Simulated Flue Gas and Ambient Air. *Energy Fuels* **2011**, *25*, 5528−5537.

(13) Choi, S.; Drese, J. H.; Eisenberger, P. M.; Jones, C. W. Application of Amine-Tethered Solid Sorbents for Direct CO_2 Capture from the Ambient Air. *Environ. Sci. Technol.* **2011**, *45*, 2420−2427.

(14) Didas, S. A.; Kulkarni, A. R.; Sholl, D. S.; Jones, C. W. Role of amine structure on carbon dioxide adsorption from ultradilute gas streams such as ambient air. *ChemSusChem* **2012**, *5*, 2058−2064.

(15) McDonald, T. M.; Lee, W. R.; Mason, J. A.; Wiers, B. M.; Hong, C. S.; Long, J. R. Capture of carbon dioxide from air and flue gas in the alkylamine-appended metal-organic framework mmen-Mg_2(dobpdc). *J. Am. Chem. Soc.* **2012**, *134*, 7056−7065.

(16) Choi, S.; Watanabe, T.; Bae, T.-H.; Sholl, D. S.; Jones, C. W. Modification of the Mg/DOBDC MOF with Amines to Enhance CO_2 Adsorption from Ultradilute Gases. *J. Phys. Chem. Lett.* **2012**, 1136−1141.

(17) Lu, W.; Yuan, D.; Sculley, J.; Zhao, D.; Krishna, R.; Zhou, H. C. Sulfonate-grafted porous polymer networks for preferential CO_2 adsorption at low pressure. *J. Am. Chem. Soc.* **2011**, *133*, 18126−18129.

(18) Lu, W.; Sculley, J. P.; Yuan, D.; Krishna, R.; Wei, Z.; Zhou, H. C. Polyamine-tethered porous polymer networks for carbon dioxide capture from flue gas. *Angew. Chem., Int. Ed.* **2012**, *51*, 7480−7484.

(19) Myers, A. L.; Prausnitz, J. M. Thermodynamics of mixed-gas adsorption. *AIChE J.* **1965**, *11*, 121−127.

(20) Mason, J. A.; Sumida, K.; Herm, Z. R.; Krishna, R.; Long, J. R. Evaluating metal-organic frameworks for post-combustion carbon dioxide capture via temperature swing adsorption. *Energy Environ. Sci.* **2011**, *4*, 3030−3040.

(21) McDonald, T. M.; D'Alessandro, D. M.; Krishna, R.; Long, J. R. Enhanced carbon dioxide capture upon incorporation of N,N'-dimethylethylenediamine in the metal-organic framework CuBTTri. *Chem. Sci.* **2011**, *2*, 2022−2028.

(22) Kizzie, A. C.; Wong-Foy, A. G.; Matzger, A. J. Effect of Humidity on the Performance of Microporous Coordination Polymers as Adsorbents for CO_2 Capture. *Langmuir* **2011**, *27*, 6368−6373.

(23) Serna-Guerrero, R.; Belmabkhout, Y.; Sayari, A. Triamine-grafted pore-expanded mesoporous silica for CO_2 capture: Effect of moisture and adsorbent regeneration strategies. *Adsorption* **2010**, *16*, 567−575.

(24) Sayari, A.; Belmabkhout, Y. Amine-Containing CO_2 Adsorbents: Dramatic Effect of Water Vapor. *J. Am. Chem. Soc.* **2010**, *132*, 6312−6314.

(25) Krishna, R.; Long, J. R. Screening Metal−Organic Frameworks by Analysis of Transient Breakthrough of Gas Mixtures in a Fixed Bed Adsorber. *J. Phys. Chem. C* **2011**, *115*, 12941−12950.

(26) Bloch, E. D.; Queen, W. L.; Krishna, R.; Zadrozny, J. M.; Brown, C. M.; Long, J. R. Hydrocarbon Separations in a Metal-Organic Framework with Open Iron(II) Coordination Sites. *Science* **2012**, *335*, 1606−1610.

(27) Wu, H.; Yao, K.; Zhu, Y.; Li, B.; Shi, Z.; Krishna, R.; Li, J. Cu-TDPAT, an rht-Type Dual-Functional Metal−Organic Framework Offering Significant Potential for Use in H_2 and Natural Gas Purification Processes Operating at High Pressures. *J. Phys. Chem. C* **2012**, *116*, 16609−16618.

(28) He, Y.; Krishna, R.; Chen, B. Metal-organic frameworks with potential for energy-efficient adsorptive separation of light hydrocarbons. *Energy Environ. Sci.* **2012**, *5*, 9107−9120.

Supporting Information for:

Carbon dioxide capture from air using amine-grafted porous polymer networks

Weigang Lu,‡[a] Julian P. Sculley,‡[a] Daqiang Yuan,[b] Rajamani Krishna,[c] and Hong-Cai Zhou*[a]

[a] Department of Chemistry, Texas A&M University, College Station, TX, 77843, USA. Tel.: +1 (979) 422-6329; Fax: (+01)979-845-1595; E-mail: zhou@mail.chem.tamu.edu

[b] State Key Laboratory of Structure Chemistry, Fujian Institute of Research on the Structure of Matter, Chinese Academy of Sciences, Fuzhou, Fujian, 350002, China

[c] Van't Hoff Institute for Molecular Sciences, University of Amsterdam, Science Park 904, 1098 XH Amsterdam, The Netherlands

‡ W. Lu and J. P. Sculley contributed equally.

Table of contents

Section	Content	Page
S1	Notation	3
S2	Pure component isotherm fits for adsorption of N_2, O_2 and CO_2 in PPN-6-CH_2Cl, PPN-6-CH_2EDA, and PPN-6-CH_2DETA	4
S3	Isosteric heats of adsorption	12
S4	Ideal Adsorption Solution Theory (IAST) calculations for mixed adsorption gas	13
S5	Breakthrough calculations	14
S6	References	17

Figures

S1	N_2 adsorption data at 295 K	6
S2	O_2 adsorption data at 295 K	7
S3	Experimental CO_2 adsorption data at 295 K in PPN-6-CH_2EDA with Langmuir isotherms for each site	9
S4	Experimental CO_2 adsorption data at 295 K in PPN-6-CH_2DETA with Langmuir isotherms for each site	10
S5	CO_2 adsorption data at 295 K and Langmuir fits for all materials	11
S6	Loading dependent isosteric heat of adsorption for all materials	12
S7	Schematic of packed bed adsorber.	15

1. Notation

b	parameter in the pure component Langmuir adsorption isotherm, Pa^{-1}
$-E$	heat of adsorption, J mol^{-1}
L	length of packed bed adsorber, m
p	bulk gas phase pressure, Pa
q	molar loading of adsorbate, mol kg^{-1}
q_{sat}	saturation loading, mol kg^{-1}
Q_{st}	isosteric heat of adsorption, J mol^{-1}
R	gas constant, 8.314 J mol^{-1} K^{-1}
t	time, s
T	temperature, K
u	superficial gas velocity, m s^{-1}

Greek letters

ε	voidage of packed bed, dimensionless
ρ	framework density, kg m^{-3}
τ	time, dimensionless
τ_{break}	breakthrough time, dimensionless

Subscripts

A	referring to site A
B	referring to site B
C	referring to site C
sat	referring to saturation conditions

2. Pure component isotherm fits for adsorption of N_2, O_2, and CO_2 in PPN-6-CH_2Cl, PPN-6-CH_2EDA, and PPN-6-CH_2DETA

Low pressure (< 800 torr) gas sorption isotherms were measured using a Micrometrics ASAP 2020 surface area and pore size analyzer. Prior to the measurements, the samples were degassed for 10 h at 120 °C. UHP grade gases were used for all measurements. Oil-free vacuum pumps and oil-free pressure regulators were used for all measurements to prevent contamination of the samples during the degassing process and isotherm measurement. Approximately 1.0 g of sample was used for all measurements.

The measured experimental isotherm data are first converted from excess loadings to absolute loadings, using information on the pore volumes along with the Peng-Robinson equation of state for estimation of the fluid density inside the pores at the prevailing temperatures and pressures. The pore volumes of PPN-6-CH_2Cl, PPN-6-CH_2EDA, and PPN-6-CH_2DETA used for this purpose were 1.0184, 0.4786, and 0.2640 $cm^3\ g^{-1}$, respectively. This conversion to absolute loadings is of vital importance for estimates of component loadings in the mixtures, and for calculation of the isosteric heats of adsorption. The need for conversion to absolute loadings has been stressed in recent publications,[1] which also underscores some commonly made errors in calculations of isosteric heats of adsorption, and the adsorption selectivities. This conversion to absolute loadings is of particular relevance for N_2 and O_2 adsorption in PPN-6-CH_2DETA, and PPN-6-CH_2EDA because the absolute loadings are about twice that of the excess loadings.

For all N_2 and O_2 adsorption there are no discernible isotherm inflections for any of structures and therefore the single-site Langmuir model (eqn. 1) was used for fitting the experimental isotherm data

$$q^0 = \frac{q_{sat} b p}{1 + bp} \tag{1}$$

The single-site Langmuir fit parameters for N_2 and O_2 are specified in Tables S1 and S2 for PPN-6-CH_2Cl, PPN-6-CH_2EDA, and PPN-6-CH_2DETA.

Table S1. Single-site Langmuir parameters for adsorption of N_2. These parameters were determined by fitting adsorption isotherms at 295 K.

	$q_{sat,A}$ mol kg^{-1}	b_A Pa^{-1}
PPN-6-CH_2Cl	0.63	2.8×10^{-6}
PPN-6-CH_2EDA	0.33	4.565×10^{-6}
PPN-6-CH_2DETA	0.1	7.647×10^{-6}

Fig. S1 compares the experimental N_2 adsorption data at 295 K for PPN-6-CH_2Cl, PPN-6-CH_2DETA, and PPN-6-CH_2EDA with the single-site Langmuir fits. Also shown in Fig. S1 are the pure component isotherm fits for N_2 adsorption in MgMOF-74, NaX zeolite, and mmen-CuBTTri (data is at 298 K) based on the parameters specified in the supporting information accompanying the publications of Mason *et al.*[2] and McDonald *et al.*[3] IAST calculations for Mg_2(dobpdc) proved to be impossible to carry out because of severe numerical difficulties associated with the 3-site Langmuir-Freundlich fit parameters provided by McDonald et al.[4] Consequently, breakthrough calculations were also not possible.It is particularly noteworthy that PPN-6-CH_2DETA has a significantly lower adsorption strength for N_2 when compared to other materials. The efficacy of PPN-6-CH_2DETA for CO_2 capture from ambient air is ascribable, in part, to the fact the extremely low adsorption for N_2; we return to this point later.

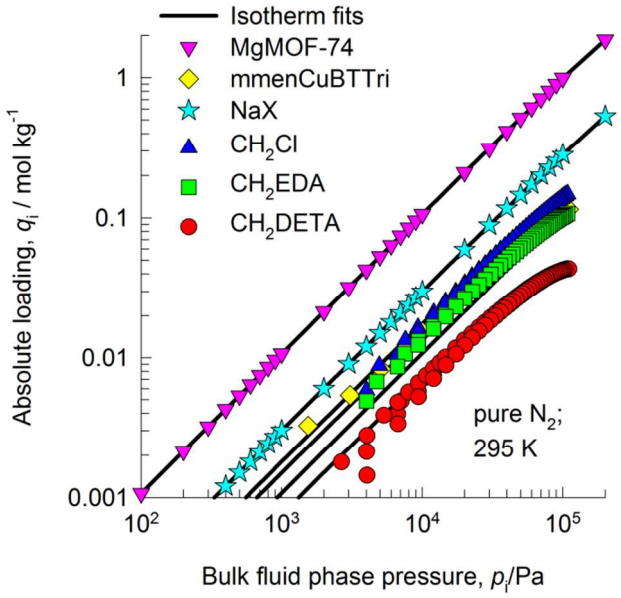

Fig. S1. Experimental N_2 adsorption data at 295 K for PPN-6-CH_2Cl, PPN-6-CH_2EDA, and PPN-6-CH_2DETA fitted with single-site Langmuir isotherm. The continuous solid lines are the single-site Langmuir fits using the parameters specified in Table S1. Also shown are the pure component isotherm fits for N_2 adsorption in MgMOF-74, NaX zeolite, and mmen-CuBTTri.

Table S2. Single-site Langmuir parameters for adsorption of O_2. These parameters were determined by fitting adsorption isotherms at 295 K.

	$q_{sat,A}$ mol kg^{-1}	b_A Pa^{-1}
PPN-6-CH_2Cl	0.28	1.059×10^{-5}
PPN-6-CH_2EDA	0.35	4.1×10^{-6}
PPN-6-CH_2DETA	0.12	7.53×10^{-6}

Fig. S2 compares the experimental O_2 adsorption data at 295 K for PPN-6-CH_2Cl, PPN-6-CH_2EDA, and PPN-6-CH_2DETA with single-site Langmuir isotherm fits. The adsorption strength of O_2 in PPN-6-CH_2DETA is comparable to that of N_2.

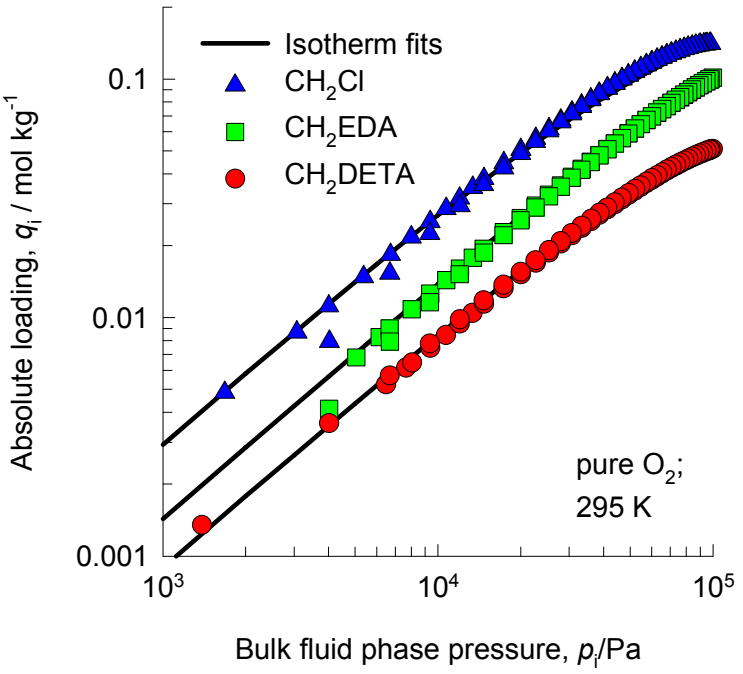

Fig. S2. Experimental O_2 adsorption data at 295 K for PPN-6-CH_2Cl, PPN-6-CH_2EDA, and PPN-6-CH_2DETA fitted with single-site Langmuir isotherm. The continuous solid lines are the single-site Langmuir fits using the parameters specified in Table S2 .

For CO_2 adsorption in PPN-6-CH_2Cl there are also no discernible isotherm inflections, therefore making the single-site Langmuir model adequate (parameters are specified in Table S3). When fitting the q_{sat} values over a range of temperatures, the q_{sat} value should be fixed because it describes the quantity of gas adsorbed when exactly one layer of a given site is saturated; this is not temperature dependent. The isotherm data, measured at 273 K, 284 K, and 295 K, were all fitted with the temperature dependence of the Langmuir constant, b, expressed as

$$b = b_0 \exp\left(\frac{E}{RT}\right) \qquad (2)$$

Table S3. Single-site Langmuir parameters for adsorption of CO_2 in PPN-6-CH_2Cl. These parameters were determined by fitting adsorption isotherms for temperatures 273 K, 284 K, and 295 K.

$$q = \frac{q_{sat} bp}{1 + bp}$$

$$q_{sat} = 10.4 \text{ mol kg}^{-1}$$

$$b = b_0 \exp\left(\frac{E}{RT}\right);$$

$$b_0 = 3.81 \times 10^{-10} \text{ Pa}^{-1}$$

$$E = 20.6 \text{ kJ mol}^{-1}$$

For CO_2 adsorption in PPN-6-CH_2EDA and PPN-6-CH_2DETA the fitting of the adsorption isotherms for the low pressure regions are of particular importance in the context of CO_2 capture from ambient air. The isotherm fits must properly capture the steep isotherm characteristics, at pressures below 1000 Pa. In our earlier work that examined CO_2 capture from flue gases, dual-site Langmuir fits were used.[5] In the current study, improved accuracy of the CO_2 isotherm fitting was obtained by adopting a triple-site Langmuir model, shown in eqn. 3.

$$q^0 \equiv q_A^0 + q_B^0 + q_C^0 = \frac{q_{sat,A} b_A p}{1 + b_A p} + \frac{q_{sat,B} b_B p}{1 + b_B p} + \frac{q_{sat,C} b_C p}{1 + b_C p} \tag{3}$$

Table S4 provides the fitted parameters for each of the three temperatures in PPN-6-CH_2EDA. The fits to experimental data are good, and this goodness-of-fit holds for all three temperatures used in the experiments. To illustrate this, Fig. S**Error! Reference source not found.** compares the experimental data for adsorption of CO_2 at 295 K in PPN-6-CH_2EDA with the triple-site Langmuir isotherm model fits. Each of the sites begins to contribute to the total loading at different regimes of pressure. For CO_2 capture from ambient, the parameters for the first site are of particular importance in determining the component loadings in mixtures with N_2 and O_2 because the partial pressures of CO_2 are typically about 40 Pa.

Table S4. Langmuir parameters of all three sites for adsorption of CO_2 in PPN-6-CH_2EDA. The data for each temperature is fitted separately.

Temperature	1st site		2nd site		3rd site	
	$q_{A,sat}$ mol kg^{-1}	b_{A0} Pa^{-1}	$q_{B,sat}$ mol kg^{-1}	b_{B0} Pa^{-1}	$q_{C,sat}$ mol kg^{-1}	b_{C0} Pa^{-1}
273 K	0.75	5.02×10^{-2}	1	1.73×10^{-3}	5.2	1.32×10^{-5}
284 K	0.75	2.44×10^{-2}	1	8.35×10^{-4}	5.2	8.16×10^{-6}
295 K	0.75	7.4×10^{-3}	1	1.84×10^{-4}	5.2	4.51×10^{-6}

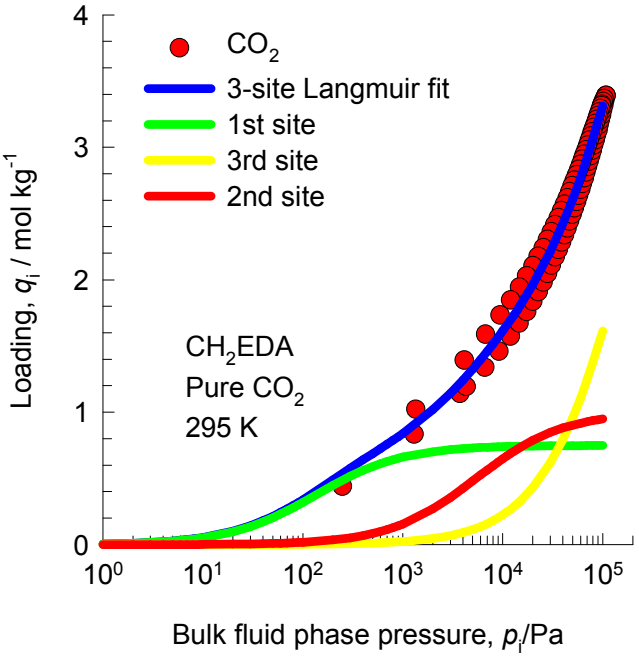

Fig. S3. Experimental CO_2 adsorption data at 295 K in PPN-6-CH_2EDA fitted with a triple-site Langmuir isotherm (blue line). The continuous solid lines represent the individual contributions of each site of the using the parameters specified in Table S4.

Table S5 shows the fitting parameters of all three sites at each temperature and Fig. S4 plots the modeled isotherms in comparison with the experimental data for PPN-6-CH_2DETA at 295 K.

Table S5. Langmuir parameters of all three sites for adsorption of CO_2 in PPN-6-CH_2DETA. The data for each temperature is fitted separately.

Temperature	1st site		2nd site		3rd site	
	$q_{A,sat}$ mol kg^{-1}	b_{A0} Pa^{-1}	$q_{B,sat}$ mol kg^{-1}	b_{B0} Pa^{-1}	$q_{C,sat}$ mol kg^{-1}	b_{C0} Pa^{-1}
273 K	1.6	2.57×10^{-1}	1.5	3.38×10^{-3}	3	2.16×10^{-5}
283 K	1.6	1.56×10^{-1}	1.5	1.33×10^{-3}	3	1.22×10^{-5}
295 K	1.6	4.38×10^{-2}	1.5	5.21×10^{-4}	3	7.1×10^{-6}

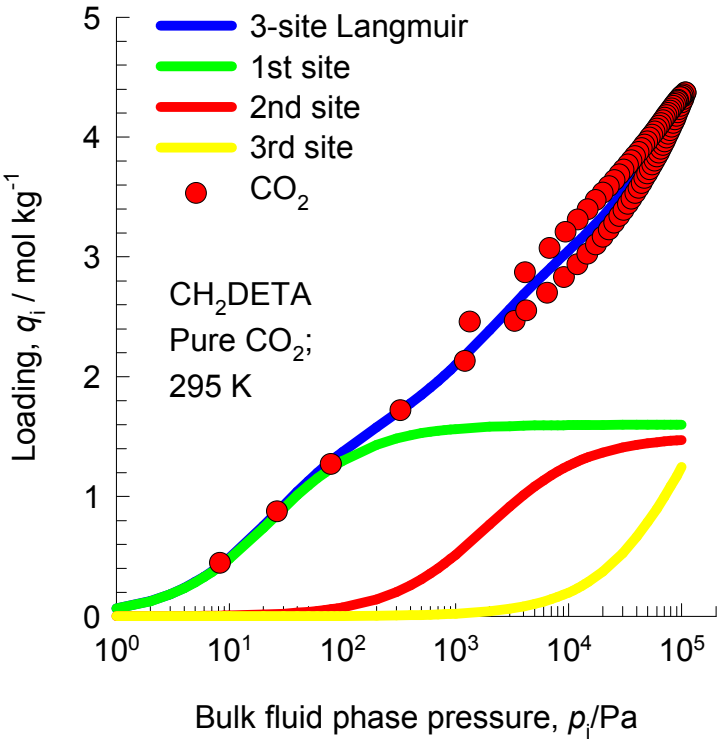

Fig. S4. Experimental CO_2 adsorption data at 295 K in PPN-6-CH_2DETA fitted with a triple-site Langmuir isotherm (blue line). The continuous solid lines represent the individual contributions of each site of the using the parameters specified in Table S5.

Fig. S5 compares the experimental data for adsorption of CO_2 at 295 K in PPN-6-CH_2Cl, PPN-6-CH_2EDA, and PPN-6-CH_2DETA with the isotherm fits using the parameters specified in Tables S3, S4, and S5. Also shown are the pure component isotherm fits for CO_2 adsorption in MgMOF-74, NaX zeolite, and mmen-CuBTTri based on the parameters specified in the publications of Mason *et al.*[2] and McDonald *et al.*[3] The most notable aspect of the isotherm data comparisons presented in Fig. S5 is that

the loadings of CO_2 in PPN-6-CH_2DETA are significantly higher than in any other structures for pressures lower than 500 Pa. This indicates the potential of using PPN-6-CH_2DETA for removing CO_2 from ambient air capture applications.

For pressures exceeding 10 kPa, the loadings of CO_2 in MgMOF-74 is higher than any other material. Indeed, for CO_2 capture from flue gas, MgMOF-74 has the highest capture capacity.[5]

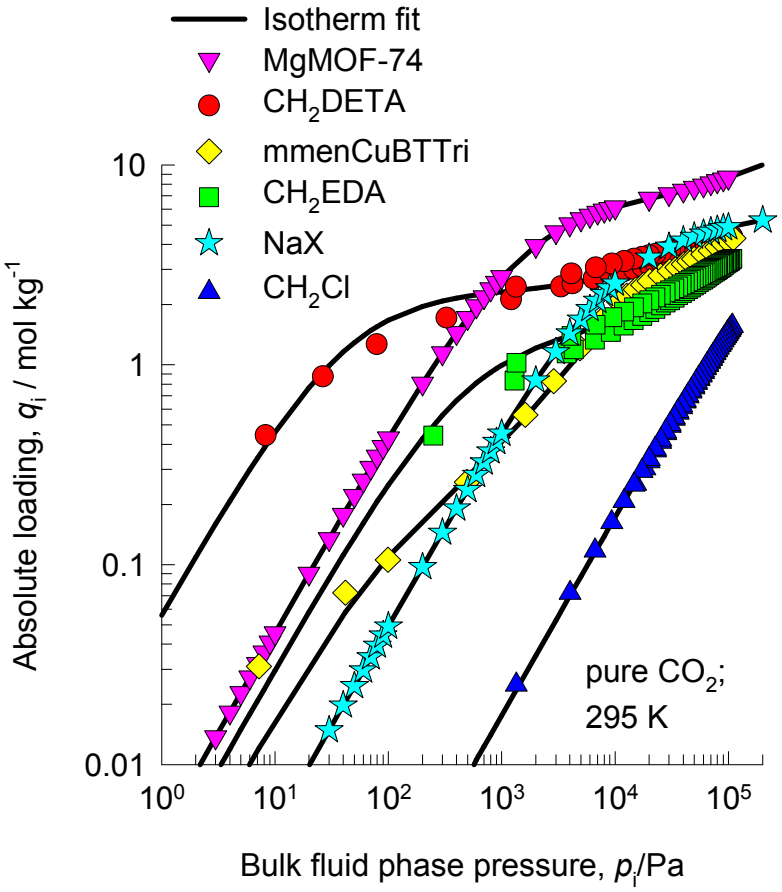

Fig. S5. Experimental data for adsorption of CO_2 at 295 K in PPN-6-CH_2Cl, PPN-6-CH_2EDA, and PPN-6-CH_2DETA. The continuous solid lines are the isotherm fits using the parameters specified in Tables S3, S4, and S5. Also shown are the pure component isotherm fits for CO_2 adsorption in MgMOF-74, NaX zeolite, and mmen-CuBTTri.

Based on elemental analysis, PPN-6-CH_2EDA has an amine loading of 0.269 amine substituents per phenyl ring, which is approximately 0.538 mol N per mol PPN-6. PPN-6-CH_2DETA has a higher loading or approximately 0.338 amines per phenyl ring, or 1.01 mol N per mol PPN-6. This in combination with the addition of a second primary amine in PPN-6-CH_2DETA imparts this analogue with a much higher CO2 loading and correspondingly higher amine efficiency.

3. Isosteric heats of adsorption

The data for each temperature is fitted separately, and the isosteric heats of adsorption, Q_{st}, is calculated by using the Clausius-Clapeyron equation.

$$Q_{st} = RT^2 \left(\frac{\partial \ln p}{\partial T} \right)_q \tag{4}$$

Fig. S6 presents data on the loading dependence of Q_{st} for the adsorption of CO_2 in PPN-6-CH_2Cl, PPN-6-CH_2EDA, PPN-6-CH_2DETA, MgMOF-74, NaX zeolite,[2] and mmen-CuBTTri.[3]

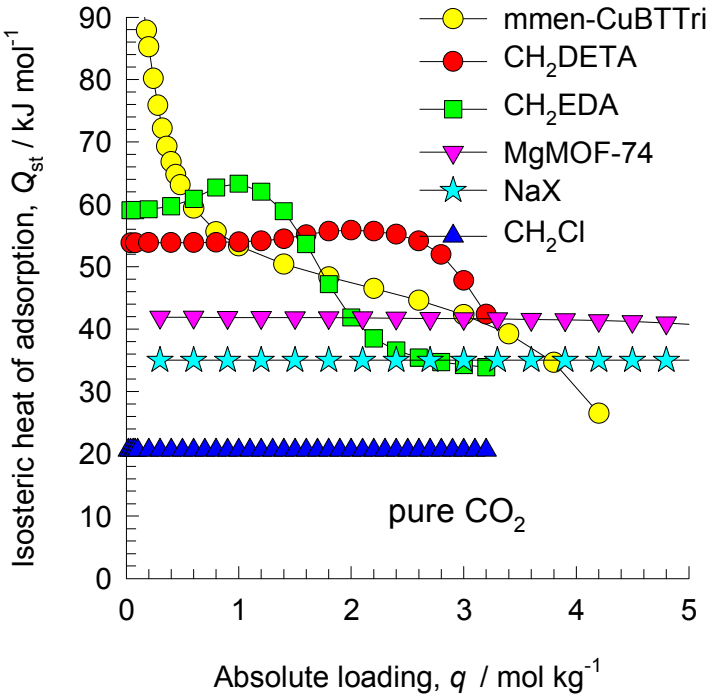

Fig. S6. The isosteric heat of adsorption, Q_{st}, for CO_2 in PPN-6-CH_2Cl, PPN-6-CH_2EDA, PPN-6-CH_2DETA, MgMOF-74, NaX zeolite, and mmen-CuBTTri.

4. IAST calculations for mixture adsorption

For mixture adsorption, the calculations of the component loadings are best carried out with the IAST. IAST calculations show greatly improved accuracy compared to ideal selectivity calculations, because adsorption from a mixture favors the component with higher saturation loading, i.e. CO_2.

IAST calculations were carried out for the following set of conditions relevant to CO_2 capture from ambient air at ambient pressures of 100 kPa.

Partial pressure of CO_2 in air = 40 Pa, corresponding to 400 ppm.

Two scenarios are considered. In the first scenario, we assume "air" to consist only of N_2, with a partial pressure of 100 kPa. In the second scenario, we take "air" to be composed of 78.96% N_2 and 21% O_2.

For the first scenario, the IAST calculations of component loadings for adsorption from the mixture are plotted given in Table S6. It is particularly noteworthy that the IAST calculations show that the N_2 loading is practically zero in PPN-6-CH_2DETA. Furthermore, the component loading for CO_2 loading in PPN-6-CH_2DETA is significantly higher than for other materials; the rationale for this can be traced to the significantly higher pure component loadings for pressures below 100 Pa, shown in Fig. S5.

The IAST calculations for the second scenario are graphically represented in the main text (Fig. 1). The component loadings of CO_2 in the adsorbed phase are hardly changed from the first scenario. Whether we consider air to be composed of 99.96% N_2, or a mixture of 78.96% N_2 and 21% O_2 does not make any significant difference to the mixture adsorption equilibrium.

Selectivity (S) is defined according to eqn. 5, while purity is defined according to eqn. 6.

$$S = \frac{q_{CO2} / q_2}{p_{CO2} / p_2} \tag{5}$$

$$purity = \frac{q_{CO2}}{q_{CO2} + q_2} \times 100\% \tag{6}$$

Table S6. Molar loadings of each gas after IAST calculation.

	molar loadings at total pressure 100 kPa			
Material	CO_2	N_2	O_2	$N_2 + O_2$
PPN-6-CH_2Cl	5.86E-4	0.104	0.0380	0.142
PPN-6-CH_2EDA	0.149	0.0582	0.0151	0.0733
PPN-6-CH_2DETA	1.04	5.37E-8	1.91E-8	7.27E-8

5. Breakthrough calculations

In order to determine whether –DETA is indeed a promising candidate for CO_2 removal from ambient air in fixed bed adsorbers, breakthrough calculations were performed using the methodology described in earlier works.[1, 6] Fig. S7 shows a schematic of a packed bed adsorber. Assuming plug flow of $CO_2(1)/N_2(2)$ gas mixture through a fixed bed maintained under isothermal conditions and negligible pressure drop, the partial pressures in the gas phase at any position and instant of time are obtained by solving the following set of partial differential equations for each of the species *i* in the gas mixture.

$$\frac{1}{RT}\varepsilon\frac{\partial p_i}{\partial t} = -\frac{1}{RT}\frac{\partial(up_i)}{\partial z} - (1-\varepsilon)\rho\frac{\partial q_i}{\partial t}; \quad i = 1,2 \tag{7}$$

In equation (7), t is the time, z is the distance along the adsorber, ρ is the framework density, ε is the bed voidage, and u is the superficial gas velocity. The molar loading of the species i, q_i, at any position z, and time t is determined from IAST calculations. Details of the numerical procedures used are available in earlier works.[6-7]

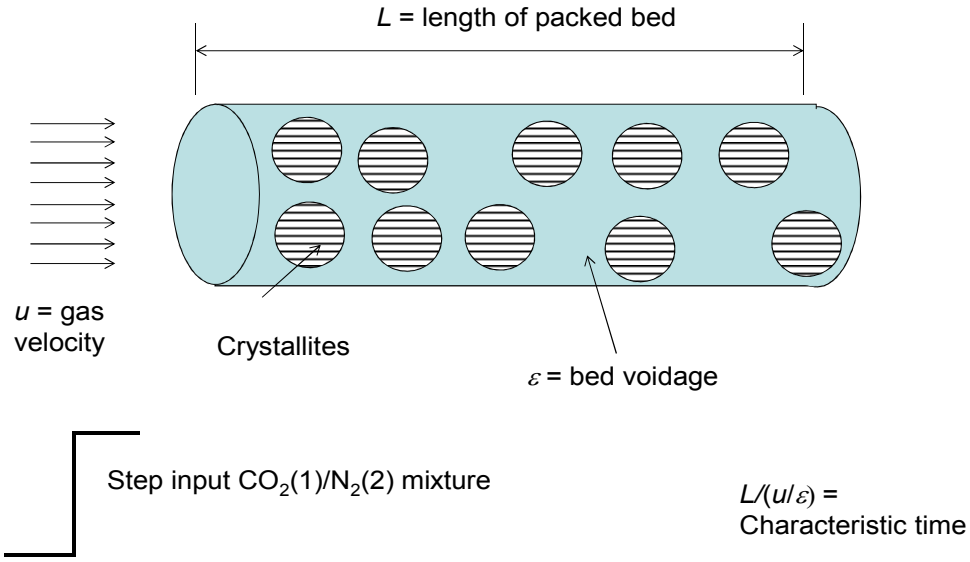

Fig. S7. Schematic of packed bed adsorber.

The breakthrough simulation methodology used here has been validated by comparison with experimental breakthrough measurements carried out by two different groups.[1b, 8]

Specifically, the calculations presented here were performed taking the following parameter values: L = 0.1 m; ε = 0.4; u = 0.04 m/s (at inlet).When comparing different materials, the fractional voidage is held constant at ε = 0.4. This implies the volume of adsorbents remains the same. The total mass of the adsorbents used is governed by the framework density. The values of the framework densities of the different materials used in the breakthrough simulations are as follows:

PPN-6-CH_2Cl: 150 kg m^{-3}

PPN-6-CH_2EDA: 300 kg m^{-3}

PPN-6-CH_2DETA: 350 kg m^{-3}

MgMOF-74: 905 kg m^{-3}

mmen-CuBTTri: 1070 kg m^{-3}

NaX: 1421 kg m^{-3}

The framework densities of PPN-6-CH_2Cl, PPN-6-CH_2EDA, and PPN-6-CH_2DETA are "tap densities", obtained from experimental determinations assuming that the solid packing fraction is 0.8. In other words, the measured tap densities are divided by 0.8.

For CO_2 capture from ambient air, the transient breakthrough characteristics are compared in main text Fig. 2. The *x*-axis is a *dimensionless* time, obtained by dividing the actual time, *t*, by the contact time between the gas and the porous materials, $\varepsilon L/u$. On the *y*-axis, the outlet gas composition in ppm CO_2 is plotted.

Longer breakthrough times are desirable, as this allows more CO_2 to be adsorbed. PPN-6-CH_2DETA has the longest breakthrough time, reflecting the highest uptake capacity for CO_2 (main text Fig. 2).

From a practical point of view, the best structure is the one that is capable of adsorbing the most amount of CO_2 for a given volume of chosen material. For this purpose we assume that the desired purity level in the CO_2 exiting the adsorber is 400 ppm. The dimensionless breakthrough time, τ_{break}, corresponding to the exit gas composition of 400 ppm CO_2 was determined for all six structures. The amount of CO_2 adsorbed during the dimensionless time interval 0 - τ_{break} was determined from a mass balance on the adsorber. The obtained values are plotted in main text Fig. 2. The capacities are calculated in terms of mol CO_2 adsorbed per L adsorbent material. Fig. 2 shows that PPN-6-CH_2DETA is significantly superior to MgMOF-74 for CO_2 removal from ambient air, and this superiority must be attributed to the significantly higher CO_2 uptake loadings at low pressures.

We also carried out breakthrough calculations for the second scenario using a mixture of 78.96% N_2, and 21% O_2 in place of 99.96% N_2. In this case, the amount of moles CO_2 adsorbed by L of PPN-6-CH_2DETA is unchanged, i.e. 0.36.

Table 7. Breakthrough time and amount of CO_2 adsorbed.

	τ_{break}	CO_2 adsorbed (mol/L)
MgMOF-74	10685	0.116
Zeolite NaX	1952.1	0.0211
mmen-CuBTTri	4053	0.0435
PPN-6-CH_2Cl	8.233	8E-5
PPN-6-CH_2EDA	3856.7	0.0418
PPN-6-CH_2DETA	33116	0.360

6. References

1. a) R. Krishna and J. M. van Baten, *Separation and Purification Technology*, 2012, **87**, 120; b) H. Wu, K. Yao, Y. Zhu, B. Li, Z. Shi, R. Krishna and J. Li, *The Journal of Physical Chemistry C*, 2012, **116**, 16609.
2. J. A. Mason, K. Sumida, Z. R. Herm, R. Krishna and J. R. Long, *Energy & Environmental Science*, 2011, **4**, 3030.
3. T. M. McDonald, D. M. D'Alessandro, R. Krishna and J. R. Long, *Chemical Science*, 2011, **2**, 2022.
4. T. M. McDonald, W. R. Lee, J. A. Mason, B. M. Wiers, C. S. Hong and J. R. Long, *J Am Chem Soc*, 2012, **134**, 7056.
5. W. Lu, J. P. Sculley, D. Yuan, R. Krishna, Z. Wei and H. C. Zhou, *Angew Chem Int Ed*, 2012, **51**, 7480.
6. R. Krishna and J. R. Long, *The Journal of Physical Chemistry C*, 2011, **115**, 12941.
7. R. Krishna and R. Baur, *Separation and Purification Technology*, 2003, **33**, 213.
8. E. D. Bloch, W. L. Queen, R. Krishna, J. M. Zadrozny, C. M. Brown and J. R. Long, *Science*, 2012, **335**, 1606.